Bulletin of Engineering Geology and the Environment
https://doi.org/10.1007/s10064-018-1234-5

ORIGINAL PAPER

Determination of the presence of microstructure in a soil using a seismic dilatometer

Dušan Berisavljević[1] · Zoran Berisavljević[2]

Received: 30 May 2017 / Accepted: 19 January 2018

Abstract
This article shows an approach for investigating the presence of microstructure in a soil based on the results obtained by seismic dilatometer (SDMT). Three main parameters are considered: intermediate dilatometer test (DMT) parameters material index (I_D) and horizontal stress index (K_D) and small strain stiffness (G_0) obtained by shear wave velocity (V_s) measurements. The approach is engineering-oriented since it is simple, fast, inexpensive, and based directly on in situ measurements. We found that with increasing microstructure (cementation and aging) the ratio of measured to estimated G_0 increases, which could be used to improve interpretation of empirically determined geotechnical parameters from DMT results. Applications of a DMT-based, CPT-based and Vs-based correlations for determination of effective peak friction angle of sands, with and without presence of microstructure, are evaluated. Finally, we propose an approach to reducing the influence of microstructure on K_0–K_D correlation in a clay.

Keywords Microstructure · Dilative · Contractive · Small strain stiffness

Introduction

Many researchers have shown that the structure significantly influences the mechanical behavior of natural and artificially prepared soil (e.g., Cotecchia and Chandler 1997; Cruz et al. 2012; Cuccovillo and Coop 1997; Gasparre and Coop 2008; Heineck et al. 2005; Mingjing Jiang et al. 2014; Pestana and Salvati 2006; Schnaid 2005; Leroueil and Vaughan 1990; Wen and Yan 2014; Yamamuro et al. 2008). Following Lambe and Whitman (1969) the term structure is used to define combination of "fabric", the arrangement of component particles, and "bonding", the interparticle forces that are not of a purely frictional nature. Generally speaking, all soils can be considered to have a structure which is more or less pronounced depending on the depositional and post-depositional processes that a particular soil has undergone during its geological life. The least pronounced structure is expected in reconstituted soils (Burland 1990), followed by natural, normally-to-lightly overconsolidated, uncemented clays, whose structure develops during one-dimensional virgin compression. The most pronounced structure develops during the various post-sedimentation processes in soil, such as unloading, aging, cementation, and their combination. Both fabric and bonding influence the mechanical behavior, but in a different manner. Heineck et al. (2005) showed that fiber reinforcement does not change the small strain stiffness (G_0), while fiber-reinforced soil has a very different behavior compared with non-reinforced soil at larger strain levels. This is explained by the greater mobilization of the tensile resistance of fibers at higher strain levels, which results in an overall strength increase of the tested soil. In reality, it is difficult to separate the effects of fabric and bonding on the mechanical behavior of soil.

Attempts have been made to quantify the influence of structure on different aspects of the behavior of clay (Cotecchia and Chandler 1997; Gasparre and Coop 2008) and sand (Consoli et al. 2007; Heineck et al. 2005). Figure 1 shows the evolution of structure in Normally consolidated (NC), young clay deposit. During deposition, the stress increase causes the volume (void ratio) to decrease. On the $\log\sigma_v$'-e diagram, deposition follows the compression curve α–α as shown in Fig. 1. After deposition, the vertical effective stress is σ_{vI}' and the void ratio is e_I. Secondary compression follows and, if the effective stress remains constant, the void ratio decreases to e_0. This decrease in void ratio can be

✉ Dušan Berisavljević
dusan.berisavljevic@sicip.co.rs

[1] Institute of Transportation CIP Ltd, 6/IV Nemanjina Street, Belgrade, Republic of Serbia

[2] Corridors of Serbia Ltd., Belgrade, Republic of Serbia

Published online: 09 February 2018

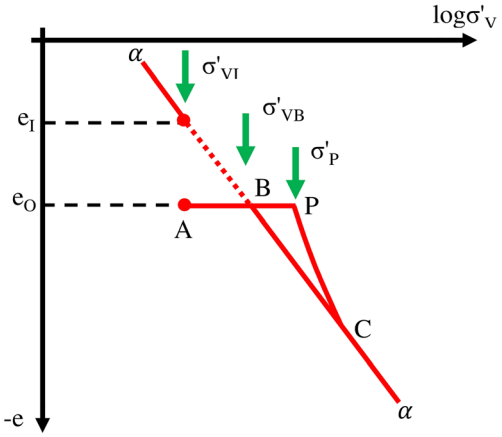

Fig. 1 Evolution of microstructure in normally consolidated clay (Leroueil and Vaughan 1990) σ'_{vI} - effective stress corresponding to void ratio e_I σ'_{vB} - apparent preconsolidation stress after secondary compression (ageing) σ'_P - apparent preconsolidation stress after cementation e_I- void ratio after deposition e_0 - void ratio after secondary compression

considered to give an apparent increase in preconsolidation stress from σ_{vI}' to σ_{vB}'. If cementation due to, for example, deposition of carbonates, iron, and aluminum oxides occurs, the apparent preconsolidation stress increases from σ_{vB}' to σ_P'. Suction also influences the apparent preconsolidation stress, where for larger suction (lower saturation degree) the elastic stress range increases and the soil behaves more stiffly (e.g., Alonso et al. 1990; Jotisankasa, et al. 2007). This apparent preconsolidation stress or yield stress represents the point where irreversible strains start to develop upon either a reduction in suction or an increase in the net total stress.

Throughout this paper, the term microstructure is used instead of structure and it is meant to describe soils that have "unusual characteristics" compared with "ideal soils" that have little or no microstructure (Robertson 2015). The major causes for the development of microstructure in soils include cementation, aging, stress, and strain history.

Soil behavior type (SBT) charts for microstructure identification

In situ penetration tests, such as the cone penetration test (CPT) or dilatometer test (DMT), are frequently used to determine the in situ mechanical response of a soil to cone penetration during CPT testing, or blade penetration and membrane expansion during DMT testing. Penetration resistance in sands is controlled by the relative density, effective stress state, compressibility and, to a lesser degree, by cementation and aging (Jamiolkowski et al. 2001; Robertson 2012). On the other hand, due to the larger number and area of grain-to-grain contact, G_0 tends to increase with increasing cementation in soil (Fernandez and Santamarina 2001; Rinaldi et al. 1998; Rinaldi and Santamarina 2008; Schnaid 2005; Schneider and Moss 2011; Viana de Fonseca et al. 2006; Yun and Santamarina 2005) and is more affected by the presence of microstructure than penetration resistance. This is mainly due to the fact that at small shear strain levels (less than 10^{-5}–10^{-6}) the bonds at interparticle contact are preserved (Diaz-Rodriguez and Santamarina 2001). The different level of sensitivity makes it possible to combine measured or interpreted large-to-medium strain parameters such as cone penetration resistance (q_c) or horizontal stress index (K_D) with small strain parameter G_0 in order to reduce the uncertainty in the application of the common correlations used to derive soil parameters. In order to do so, it is important to identify the presence of microstructure in a soil. A useful chart for identifying the presence of cementation in a soil was proposed by Cruz et al. (2012). Based on the large international database for sedimentary soils and a limited number of datapoints for granitic residual soils, Cruz et al. (2012) interpreted that cemented residual soils can be discerned from sedimentary low or non-cemented soils based on consideration of the G_0/ dilatometer modulus (E_D) versus material index (I_D) or G_0/ DMT constrained modulus (M_{DMT}) versus K_D correlations. Another useful chart which may have a potential to identify the presence of microstructure in soil was proposed by Rivera-Cruz et al. (2012). The chart consists of seven zones representing different soil behavior types, as shown in Fig. 2. The major drawback of this chart is the need to measure the p_2 pressure, which significantly extends the time needed to perform the test.

Both the previously mentioned charts consider either the G_0/E_D or G_0/M_{DMT} ratio together with one of the intermediate parameters in order to determine the presence of microstructure. Robertson (2015) presented a DMT-based soil behavior

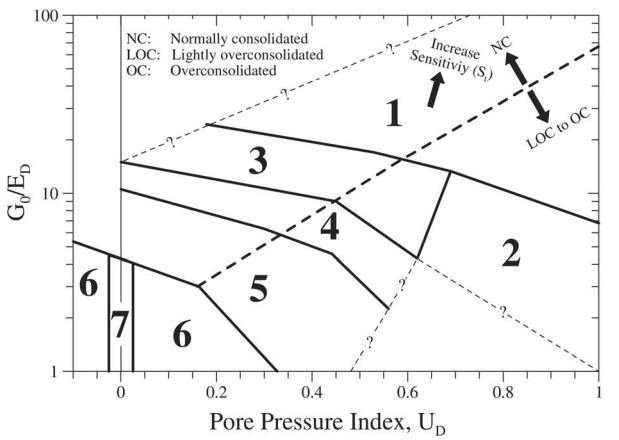

Zone	*SBT	Zone	*SBT
1	Sensitive clay to silty clay	5	Silt to sandy silt
2	Clay to silty clay	6	Silty sand
3	Silty clay	7	Sand
4	Clayey silt to silt		

*SBT: Soil behaviour type

Fig. 2 Seismic dilatometer (SDMT)-based soil behavior type chart (Rivera-Cruz et al. 2012)

type chart that considers intermediate DMT parameters I_D and K_D with the addition of the contours of the G_0/σ_v' ratio. In this paper the DMT-based soil behavior type (SBT) chart presented by Robertson (2015) is extended and validated for various soil types.

This research is based on two concepts. First is the measured to estimated G0 ratio (MEGR), which takes into consideration the measured to estimated G_0 (G_0/σ_v') ratio for microstructure identification. This concept is similar to the measured to estimated velocity (Vs) ratio (MEVR) used to correct liquefaction resistance for aged sands presented by Andrus et al. (2009) and Hayati and Andrus (2009). The second concept is based on the idea presented by Robertson (2015) at the recently held DMT'15 conference. The DMT performance and derivation of parameters can be found in Marchetti (2001).

Estimation of shear wave velocity (V_S) from seismic dilatometer (SDMT) correlations

When no seismic data are available during geotechnical investigations, it is possible to estimate shear wave velocity (V_s) from the seismic dilatometer (SDMT)-based correlations derived by Marchetti et al. (2008), which are shown in Fig. 3.

Most empirical correlations for penetration tests are based on case histories from soils with little or no microstructure (Robertson 2015); thus, when using such correlations engineers need to be cautious since G_0 in highly structured soil can be underestimated. Subsequent validation of these correlations has shown that the relative error in the estimated V_s (from I_D, K_D, and M_{DMT}) is on average 20% (Marchetti 2014). As previously mentioned, the measured V_s (G_0) is highly sensitive to the presence of microstructure in soil. Thus, comparison between the measured and estimated velocity can be directly used to

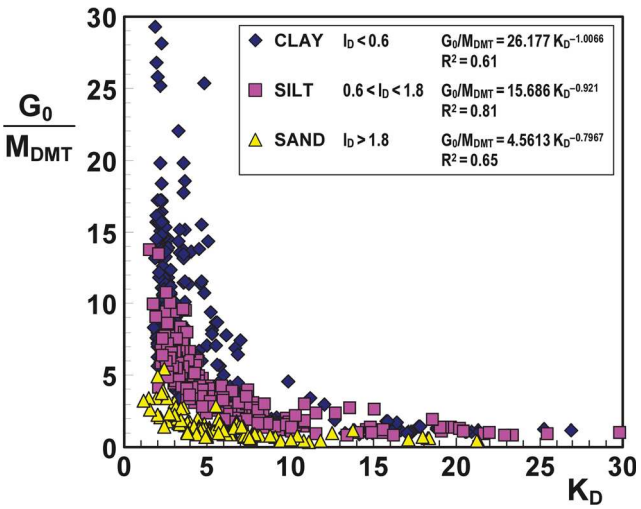

Fig. 3 Ratio of G_0/M_{DMT} vs. K_D (overconsolidation ratio [OCR]) for various soil types (Monaco et al. 2009). *G_0* small strain stiffness

detect soils that behave differently from "ideal" soils, i.e., soils without significant presence of microstructure. Figure 4 shows a comparison between the measured and estimated (from correlations shown in Fig. 3) V_s profiles for five sites.

The presence of microstructure is estimated indirectly based on geological evidence and the history of the deposit, and directly based on core sample inspection and laboratory test results when available. During drilling, visual inspection and HCl acid was used on core samples in order to check the presence of carbonates. A brief description and estimation of the level of microstructure for the first site (Vrbas I) located near the town of Vrbas is given here. The topmost layer (first meter) is desiccated crust, and according to the Unified Soil Classification System (USCS) it is classified as CL with a degree of saturation of 90%. Below the desiccated crust, 1.0 m of aquatic loess is found underlain by 2.0 m of saturated clayey silt of low plasticity. Below the clayey silt, silt of low plasticity, 2.5 m thick, is found. The water level is at a depth of 4.0 m from the ground surface. Beneath the low plastic silts, fine silty sand with 15% fines is encountered. The thickness of this layer is on average 1.8 m and it is underlain by a layer of fine-to-medium coarse, quartz, alluvial sand, which is normally consolidated with an M_{DMT}/q_c ratio of approximately 6. Its overall thickness is large and it was not determined during field investigations.

From Fig. 4a it can be observed that the estimated velocity closely follows the measured velocity except at depths from 6.0 to 8.0 m, where the fine silty sand layer is encountered. In this layer, the average relative error between the measured and estimated V_s is 40%, which is twice the average error reported by Marchetti (2014). It can be assumed that this difference is due to the presence of microstructure in the fine silty sand. Two possible factors may have caused microstructure to develop in this layer. Firstly, it was deposited in a slow-moving or stagnant water environment, which is evident from the presence of organic matter and finer particles than the sand layer below, which is typical river bed sediment of the Danube River. Secondly, it is believed that precipitation of carbonates from upper layers caused cementation of the soil particles.

Figure 4b shows the measured and estimated V_s for another site located near the town of Vrbas (Vrbas II site). The location of this site is approximately 3.5 km from the Vrbas I site. It consists of alluvial deposits. The upper 9 m consist of silts interbedded with fine silty sands. The lower soil layer consists of predominantly quartz sand, which belongs to the same geological unit as the sand described for the previous site. At this site, no significant presence of microstructure is found. From Fig. 4b, it is observed that the measured and estimated velocities closely match, except where local peaks in the estimated velocities are encountered. These peaks are usually difficult to detect from the measured velocity, since it is average in 50 cm while K_D and I_D are determined at 20 cm depth intervals. Figure 4c presents the results of measured and estimated V_s for the Loznica site, where terrace sediments (upper 10.0 m)

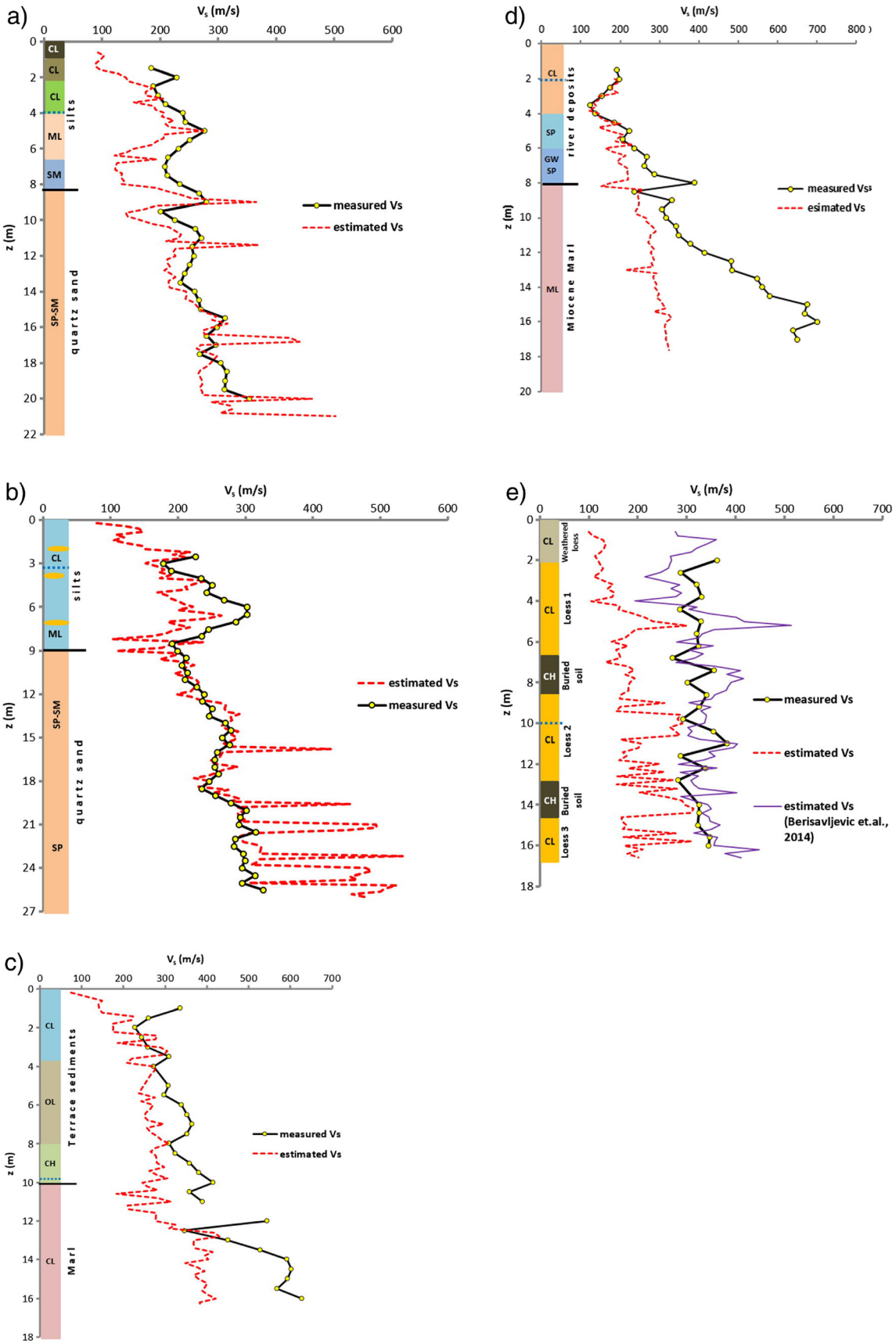

Fig. 4 Comparison between the measured and estimated shear wave velocity (V_s) profiles: (**a**) Vrbas I site, (**b**) Vrbas II site, (**c**) Loznica site, (**d**) Obrenovac site, and (**e**) Zemun loess

are underlain by stiff marls. The water level is at a depth of 10.0 m. The measured and estimated velocities differ significantly, particularly below the depth of 4.0 m. Below this depth, field investigations of terrace sediments have confirmed the presence of organic matter and carbonates. The influence of the suction on the measured velocities and DMT pressures in the layers above the water table is not known, but it is believed that it can be significant. The average relative error in the estimated velocity for marls is more than 25%. This is an expected result for marl, which is a soil with a significant presence of microstructure due to cementation. It is worth noting that during testing of these marls a limit pressure of 80 bars was reached on the high pressure gauge of the DMT control unit. It could be postulated that the high effective stress state reduces the effect that cementation has on the measured V_s (Rinaldi et.al. 1998; Yun and Santamarina 2005; Pestana and Salvati 2006; Rinaldi and Santamarina 2008) and that the difference between the measured and estimated V_s could be expected to be even greater in less overconsolidated marls. In order to confirm that, the results for another site (Obrenovac) where marls were tested are shown in Fig. 4d. The ground profile at this site consists of an 8.0 m thick alluvial deposit underlain by marl. From the figure it can be seen that the measured and estimated velocities diverge more rapidly at the depth where marls are encountered (approximately 8.0 m). This confirms that the measured velocities are highly influenced by the presence of microstructure in the soil. The difference in the measured and estimated velocities from 6.0 to 8.0 m is possibly due to the fact that at those depths the tests were performed in sandy gravels where the use of DMT may not be suitable (Marchetti et al. 2001). The derived DMT parameters (M_{DMT} and K_D) thus yield a poor prediction of V_s in gravelly soils. Figure 4e shows the velocity profile obtained in loess. A description of this site can be found in Berisavljevic et al. (2014 and 2015). By its nature, this loess is highly structured. The measured V_s profile is approximately constant with depth, with no difference between the buried soil and loess horizons. On the other hand, the estimated velocity profile gradually increases from the ground surface and has several marked peaks. Closer inspection of the correlation used to estimate V_s reveals that these peaks are a consequence of the greater difference between p_1 and p_0, i.e., a larger DMT modulus E_D. It was found by Berisavljevic et al. (2014) that p_0 (K_D) is very low and consequently any variation in p_1 may produce a significant difference in E_D and thus M_{DMT}, which is used to derive G_0 from the correlations shown in Fig. 3. A much better prediction of V_s is obtained when the correlation proposed by Berisavljevic et al. (2014) is used, as shown in Fig. 4e.

The observed results indicate that:

- correlations for estimating V_s from DMT results are derived for soils without a significant presence of microstructure;
- the larger the difference between measured and estimated velocity, the greater is the presence of microstructure in soil; and
- correlations shown in Fig. 3 should be used with caution when there is an indication that the soil is structured.

When SDMT data for gravels exist, the reverse methodology may apply. It is possible to estimate K_D from thrust measurements (F_{DMT}) at the surface using the relation proposed by Campanella and Robertson (1991) between the effective lift-off pressure (p_0-u_0) and F_{DMT}. Then, the measured V_s can be used to derive G_0 by introducing the mass density (which is usually not difficult to estimate correctly). Knowing both K_D and G_0, it is possible to estimate M_{DMT} from Fig. 3 (for $I_D > 1.8$). It is believed that this approach is more appropriate for the estimation of M_{DMT} in gravels, even if correlations between (p_0-u_0) and F_{DMT} and G_0/M_{DMT} and K_D are derived for sands. This approach is supported by the fact that the total thrust (blade penetration resistance q_D) increases when the blade is penetrating through gravels, while p_0 decreases compared to sands in the same geological unit. This approach is strongly influenced by the mean grain size diameter (D_{50}). Nevertheless, the proposed approach needs further investigation.

Microstructure-soil behavior type (M-SBT) chart

Figure 5 shows the proposed microstructure-soil behavior type (M-SBT) chart.

On the chart, four broad groups of soil behavior are distinguished: FC—fine-grained contractive, FD—fine-grained dilative, CC—coarse-grained contractive, and CD—coarse-grained dilative. These groups differentiate soil types that differ in their mechanical response to blade penetration and membrane expansion during a DMT. For instance, when testing highly overconsolidated clays, the tendency of the clay to dilate is restricted due to low permeability, which can cause negative (lower than hydrostatic) pore pressures to develop, thus increasing the effective stress in the soil and mobilizing the frictional shearing resistance. A soil with this response will fall into the FD zone. Based on the value of I_D, the soil can be classified as fine-grained ($I_D < 0.6$) or coarse-grained ($I_D > 1.8$). Fine-grained soils would have an undrained response during a DMT, while coarse-grained soils would have a drained response during a DMT. Partial drainage may take place in transitional soils, i.e., in the intermediate permeability range ($0.6 < I_D < 1.8$), as suggested by Schnaid and Odebrecht (2015). The boundary between dilative and contractive behavior is proposed by Robertson (2012) for soils with little or no microstructure. For fine-grained soils, the boundary

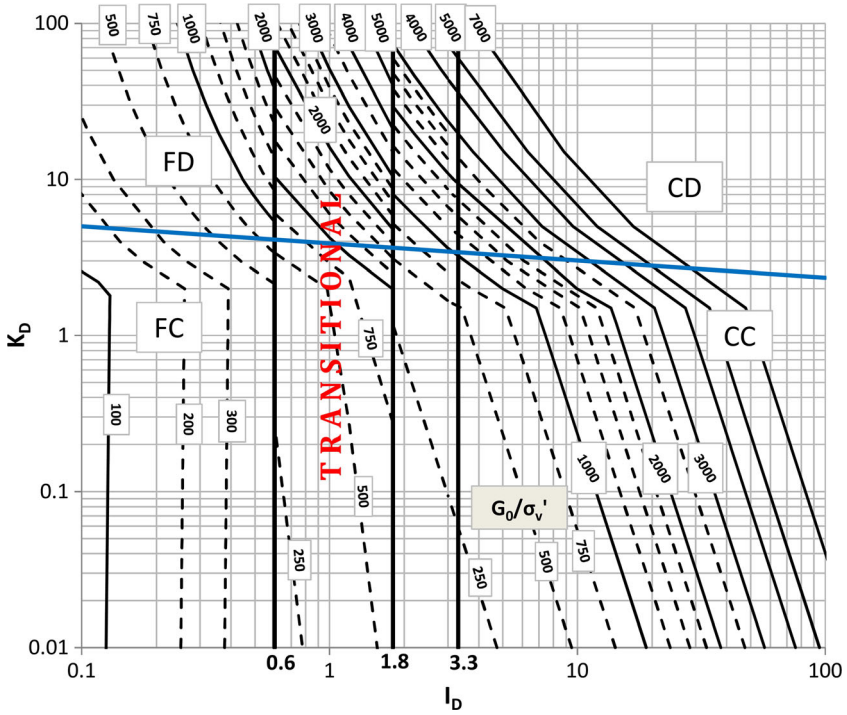

Fig. 5 Proposed microstructure-soil behavior type (M-SBT) chart

between dilative and contractive behavior at large strains occurs when the over consolidation ratio (OCR) ≈ 4. Based on Marchetti et al. (2001), the correlation value of OCR = 4 corresponds to $K_D \approx 5$. For coarse-grained soils, the boundary between dilative and contractive behavior at large strains occurs for state parameter $\psi \approx -0.05$ (Robertson 2012). Derivation of the state parameter to be used for constructing the boundary between dilative and contractive behavior for coarse-grained soils is a two-step process. First, the state parameter is derived from CPT-based correlations with clean sand equivalent normalized cone resistance ($Q_{tn,cs}$) (Robertson 2010). Secondly, the link between K_D and $Q_{tn,cs}$ is used with the $Q_{tn,cs} - \psi$ correlation (Robertson 2012) to obtain the following equation:

$$\Psi = 0.56 - 0.33 \cdot log(25 \cdot K_D) \quad (1)$$

In Eq. 1, $K_D = 3$ yields $\psi \approx -0.05$, which defines the contractive–dilative boundary for coarse-grained soils. As suggested by Robertson (2015), this boundary is not defined by a single value of K_D for all soils. It should be mentioned that the contractive–dilative boundary is linearly extrapolated with the same slope from $I_D = 10$ to the practically impossible value of $I_D = 100$. This extension of the boundaries of the SBT chart given by Robertson (2015) is mainly due to the clearer presentation of the data and completeness of the chart. The presence of microstructure in the soil is estimated by comparing the measured and estimated G_0/σ_v' ratios. The contours of the G_0/σ_v' ratio are derived by linking the correlations presented in Fig. 3 and correlations for M_{DMT} as proposed by Marchetti (1980) and Marchetti et al. (2001). The contours of the G_0/σ_v' ratio are plotted on the M-SBT chart shown in Fig. 5.

Validation of M-SBT chart

Figures 6, 8, and 9 show results obtained in various soil types plotted on the M-SBT chart. On each chart a brief description of the tested soil is included. Minimum and maximum values as well as the arithmetic mean (given in parentheses) of the measured G_0/σ_v' ratio for the particular soil are given. The arithmetic mean and the range of values give one possible way to compare the measured and estimated data for a particular soil. The stricter and more precise approach would be to compare the measured and estimated values for each datapoint, but this is less convenient for presentation in graphical form when a large amount of data are evaluated. It should be mentioned that G_0 evaluated from SDMT is obtained from a measured "true interval" velocity (every 0.5 m), so the equivalent value of I_D and K_D should also be taken as an average of three successive readings at a depth corresponding to the G_0 evaluation. The position of each point shown on the M-SBT chart is determined from the average I_D and K_D values of three successive readings, which differ by less than 10%.

Fine-grained soils

Figure 6 presents the results for fine-grained soils. It is interesting to compare the Fiumicino clay and Smederevo silty

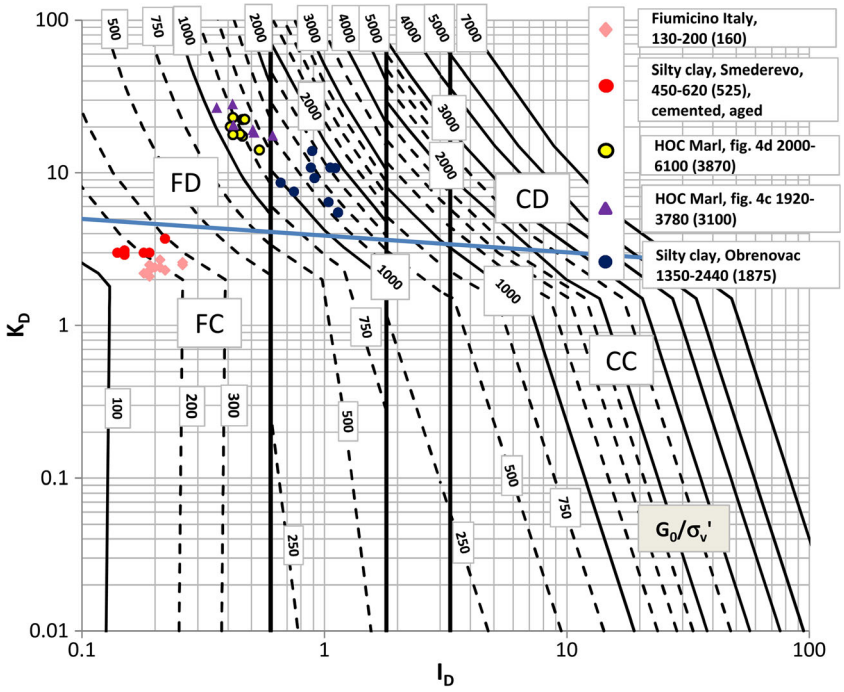

Fig. 6 Validation of proposed microstructure-soil behavior type (M-SBT) chart: fine-grained soils ($I_D < 0.6$) and transitional soils

clay both plotted in the FC region lying relatively close to each other. The datapoints for both soils plot on the same "estimated" G_0/σ_v' lines but the Smederevo silty clay has a significantly higher "measured" G_0/σ_v' ratio. This may indicate that the behavior of the silty clay is influenced by the presence of microstructure. It is believed that the microstructure is caused by cementation and aging, as indicated in the legend of Fig. 6. Cementation could be a consequence of the high carbonate content (24%) measured in the laboratory. Marchetti et al. (2001) suggested that cemented clays can be

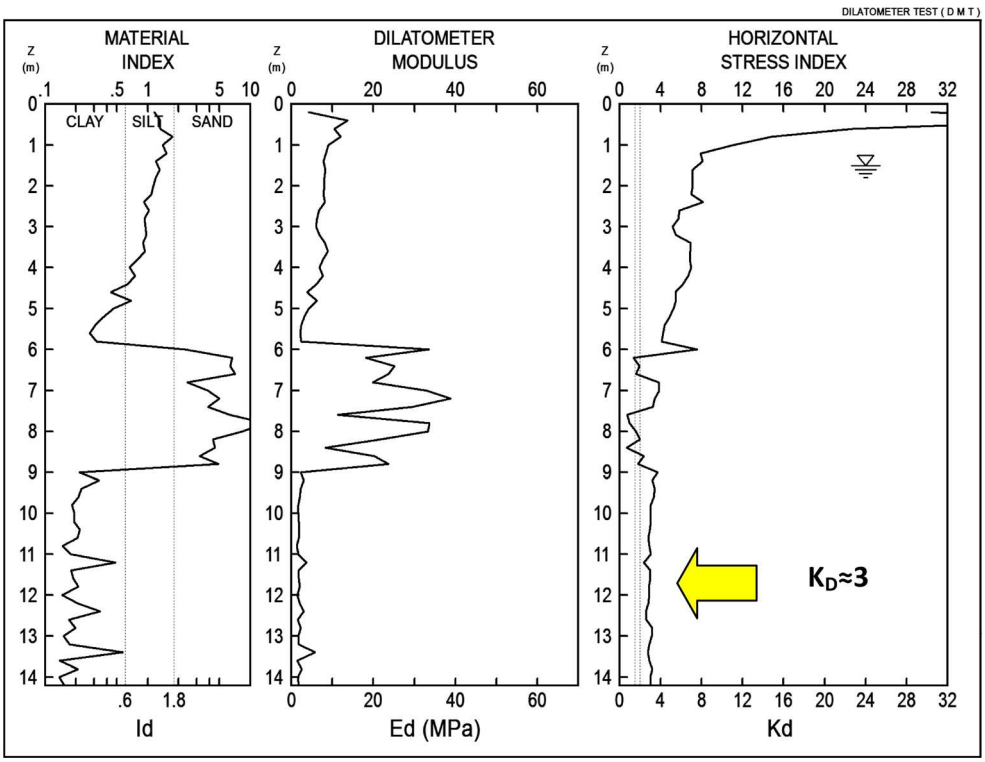

Fig. 7 Profiles of intermediate dilatometer test (DMT) parameters for Smederevo silty clay (depth below 9.0 m)

recognized by a constant value of K_D (K_D = 3–4) with depth. For Smederevo silty clays, K_D is approximately equal to 3 and is constant with depth, as shown in Fig. 7.

As presented on the M-SBT chart in Fig. 6, points for marl (HOC marl) plot in the FD region, which could be a consequence of the high apparent overconsolidation. The estimated average G_0/σ_v' ratio for both marls is more than two times lower than the average measured G_0/σ_v' ratio. This is expected due to the presence of cementation in marls. Based on the previous two groups of soil discussed, the M-SBT chart shows a strong potential to accurately identify soil types based on their mechanical response to blade penetration in the DMT. The last soil included in the chart given in Fig. 6 is Obrenovac stiff silty clay, which is found above water level at relatively shallow depths (3–7 m) from ground elevation. Subsequent laboratory testing on samples retrieved from boreholes indicated almost full saturation of this soil ($S_r > 95\%$). Thus, it could be expected that suction has a negligible influence on the measured V_s and G_0. Datapoints for this soil plot in the transitional zone, e.g., $0.6 < I_D < 1.8$, which could indicate that the measured DMT pressures are influenced by partial drainage of pore pressures during the test (Schnaid and Odebrech, 2015). Unfortunately, during the test, the C reading and/or short dissipation tests (as suggested by Marchetti 2015) were not performed in order to determine the influence of partial drainage on the measured DMT pressures. However, high K_D values could indicate the dilative nature of this stiff clay. The measured and estimated G_0/σ_v' ratios differ on average by 20%, which is much less than for the previously presented soil types. This is consistent with field observations and laboratory testing, where no significant presence of microstructure is found in this soil.

Coarse-grained soils

The results obtained in coarse-grained soils ($I_D > 1.8$) are presented in Fig. 8. The three sands presented are normally consolidated, two of which are clean quartz alluvial sands (≈88% quartz) belonging to the same geological unit (Vrbas I and Vrbas II). For quartz sands, a close match between the measured and estimated G_0/σ_v' ratios is observed. The average estimated G_0/σ_v' ratio for the sand at the Vrbas I site is approximately 800, while the average measured ratio is 1070. The relative difference between the average measured and average estimated G_0/σ_v' ratios is approximately 25%. When assessing the presence of microstructure in soil from the G_0/σ_v' ratio, a larger relative difference should be allowed than when estimating it from the V_s ratio, since G_0 is derived from the square of the measured velocity. Thus, it is believed that the 25% relative difference is common and to be expected for soils without any significant presence of microstructure. The trends shown in Fig. 3 are derived for the global database (Marchetti et al. 2008; Monaco et al. 2009), but some variability should still be allowed due to the local soil conditions. For the Vrbas II sand, the estimated and measured G_0/σ_v' ratios closely match, as can be observed from Fig. 8. This is expected and consistent with the trends shown in Fig. 4b. Most datapoints for both sands lie above the contractive–dilative boundary, indicating a dilative behavior (negative state parameter) during drained loading. The NC silty sand site is located near the city of Subotica in the northern part of Serbia. The results correspond to the data obtained at depths ranging from 19 to 25 m below ground level measured in two SDMTs. Subotica sand is rich in carbonates, as was observed from inspection of core samples using HCl acid. As a consequence of a high carbonate content, the sand is colored white. Lower cone penetration resistances (q_c) and thrust measurements (i.e., q_D) at a similar stress level (i.e., similar depth of testing) may indicate the higher compressibility of Subotica sand than previously described quartz sands, which on the other hand may indicate that this sand has a different mineralogy. Unfortunately, no systematic research has been conducted in order to inspect the mineralogical composition of this sand more closely. The field observations and SDMT results indicate that the silty sand is cemented but that its structure is very sensitive to disturbance produced by large shear strains imposed during blade (or cone) penetration. On the other hand, small strains imposed during propagation of shear waves keep the structure intact. These observations are reflected in the large difference (on average 2.3 times) between the measured and estimated G_0/σ_v' ratios. Even if the contractive–dilative boundary, shown in Fig. 8, is determined for young soils without significant microstructure (Robertson 2015), it is believed that the contractive behavior of Subotica sand determined from the M-SBT chart corresponds to the expected behavior.

Loess and loess-like soils

Figure 9 presents a M-SBT chart including the results obtained for various soil types. These results are taken either from the literature or from the author's database.

In light of the DMT results, collapsible loess behaves as a sand-like soil (Berisavljevic et al. 2014; Lutenegger and Donchev 1983; Mulabdic and Minazek 2015). On the M-SBT chart data, points for loess plot in the CC region far below the contractive–dilative boundary. This indicates that at higher strain (stress) levels, which cause the loess structure to collapse, loess has a contractive behavior. Most of the datapoints of the estimated G_0/σ_v' ratio lie below the G_0/σ_v' = 750 line, while the measured ratios are significantly higher, ranging from 1090 to 4380. The high measured G_0/σ_v' ratios are a consequence of the larger grain-to-grain contact area produced by cementation of the larger silt and sand particles with clay minerals and $CaCO_3$. Thus, large differences in the measured and estimated ratios are a clear indicator of the presence of microstructure in the soil. A description of the loess sites

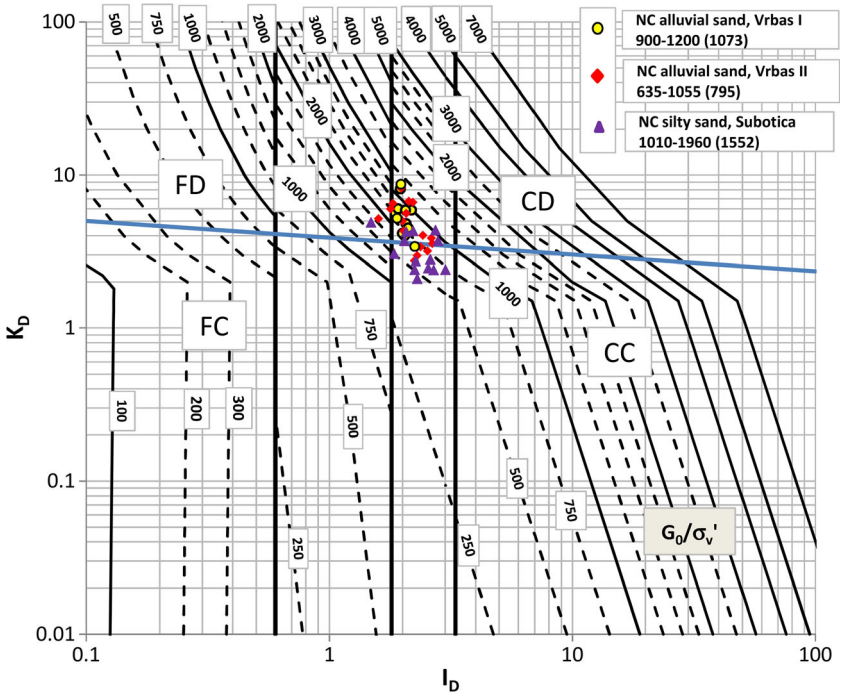

Fig. 8 Validation of proposed microstructure-soil behavior type (M-SBT) chart: coarse-grained soils ($I_D > 1.8$)

presented herein can be found in Berisavljevic et al. (2014 and 2015). Beside Serbian loess, other loess-like soils are included on the M-SBT chart shown in Fig. 9.

The results reported by Mlynarek et al. (2015) represent non-collapsible, normally consolidated loess silts with G_0/σ_v' ratios ranging from 500 to 850. The area marked in Fig. 9 indicates the range of I_D and K_D values estimated from charts reported by Mlynarek et al. (2015). The location of the marked area allows determination of the estimated G_0/σ_v' ratio. It can be observed that the estimated and measured G_0/σ_v' ratios closely match, which is consistent with findings reported by Mlynarek et al. (2015). Datapoints before and after wetting for Spanish loess-like soil reported by Devincenzi and Canicio (2001) are included in the chart. The presented results indicate that soil before wetting behaves as coarse-grained dilative (CD region), while after wetting it behaves as coarse-

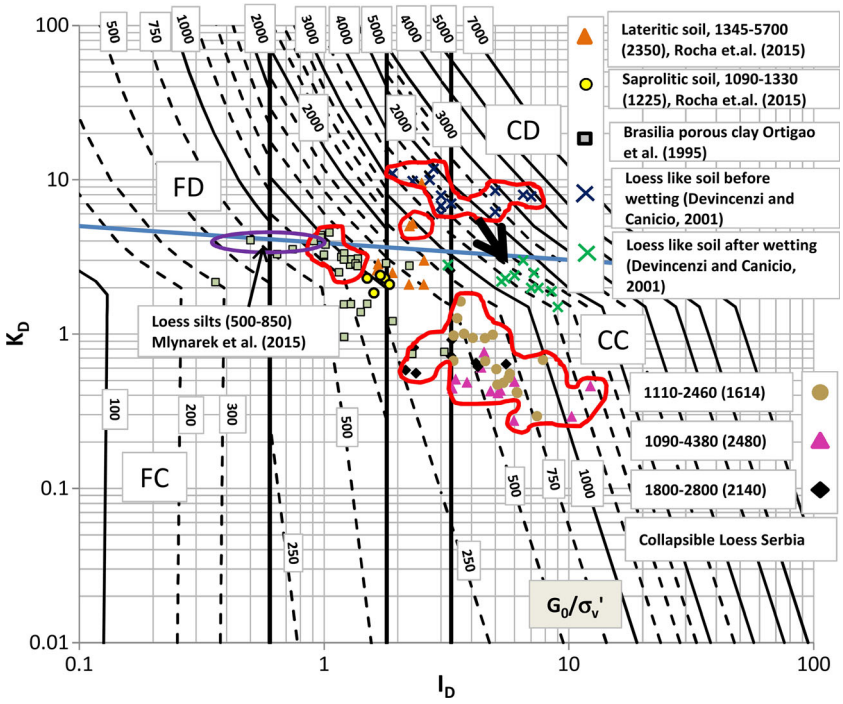

Fig. 9 Validation of proposed microstructure-soil behavior type (M-SBT) chart: various soil types. G_0 small strain stiffness

grained contractive (CC). The change of position on the M-SBT chart is a direct consequence of soil structure collapse caused by wetting of the soil. In the pre-wetted state, the cohesion (cementation) contribution causes high apparent overconsolidation, which is reflected in the dilative behavior similar to dense sand. After saturation, this cementation is lost, which causes the soil to behave as NC loose sand. It is interesting to note that the Serbian loess and loess silts reported by Devincenzi and Canicio (2001) behave as a sand-like soil even if both soil types have high fines content (> 85%). When tested at natural moisture content (for both soils the degree of saturation is approximately 50%), these soils show significantly different behavior, as can be seen from their positions on the M-SBT chart, i.e., the loess-like silts plot far above the contractive–dilative boundary, while Serbian loess plots far below it for a similar range of I_D ($I_D > 1.8$). A possible explanation of this opposite behavior of these two loess soils can be sought in the different values of their natural void ratio (e_0). Devincenzi and Canicio (2001) reported that e_0 for tested loess-like soil ranges from 0.6 to 0.7, while for Serbian loess e_0 ranges from 1 to 1.2. This may imply that Serbian loess is much more sensitive to disturbance caused by blade penetration. Thus, in sensitive loess the soil around the blade collapses, and is displaced further away from the blade. Consequently, the pressures taken in the DMT reflect the result of a soil tested in a completely disturbed state providing excessively low values of K_D. On the other hand, DMT pressures in less sensitive loess are taken in soil with partially preserved structure, giving a result that represents "real" soil behavior.

Tropical soils

The results reported by Ortigao (1994), Ortigao et al. (1995), and Rocha et al. (2015) for tropical soils are shown on the M-SBT chart given in Fig. 9. Brasilia porous clay falls into the transitional soil region, which may indicate difficulties in the derivation of geotechnical parameters from the usual interpretation formulae (e.g., Marchetti et al. 2001). This soil has a high void ratio (1.7) and low dry densities produced by the laterization process, particularly in the top layers. As reported by Ortigao et al. (1995), this clay is collapsible, which is indicated by the red boundary on the SBT chart. G_0 was not reported for this site . Recently, Rocha et al. (2015) presented the results of SDMT performed in lateritic and saprolitic soils. Datapoints for the Bauru RS2 site are shown in Fig. 9. Rocha et al. (2015) reported that the mechanical behavior of lateritic and saprolitic soil differs significantly. The SBT chart recognizes this difference in behavior, which can be seen from the different locations of points representing both soil types. Moreover, the measured G_0/σ_v' ratio is much higher in lateritic than in saprolitic soil. The trend of G_0/σ_v' to decrease with depth is similar to the evolution of the laterization process from the ground surface toward deeper layers. This similarity shows the potential of determining the extent of lateritic soil from the measured G_0/σ_v' ratio. Based on the findings reported by Giacheti et al. (2006) for the Bauru site, it seems that the G_0/σ_v' ratio is a better parameter than G_0/E_D for distinguishing lateritic from saprolitic soil.

A final observation regarding the position of collapsible soil on the M-SBT chart can be made. Datapoints which are known to represent collapsible soil from the author's database as well as soils reported in the literature are bonded by a red line. For Brasilia porous clay, the datapoints for the top 8 m are believed to represent potentially collapsible soil. Collapsibility is assessed from the dry unit weight, void ratio, and moisture content taken or evaluated from figures reported by Ortigao (1994) and Ortigao et al. (1995). For lateritic soil, it is assumed that the topmost 4 m are collapsible. From Fig. 9, it can be observed that no single position of collapsible soil exists in the M-SBT chart. This signifies the importance of geotechnical investigations, site characterization, and complexity in various soil type identifications based on their mechanical behavior during penetration testing. It should be mentioned that all the datapoints presented on the M-SBT charts taken from the literature have approximate positions, since they are read or digitized from graphs reported in the mentioned references.

Trends of small strain stiffness (G_0) with intermediate dilatometer test (DMT) parameters

The well-documented trend that G_0 normalized with respect to one of the DMT-derived parameters, such as E_D or M_{DMT}, decreases with increasing K_D or I_D has been previously reported (Marchetti 2008; Monaco et al. 2009; Cruz et al. 2012; Rivera-Cruz et al. 2012). Figure 10a shows trends of the ratio of measured to estimated small strain shear moduli ($G_{measured}/G_{estimated}$) with K_D for soils with $I_D > 1.8$. Datapoints for Aveiro sand taken from graphs reported by Amoroso et al. (2015) are added beside the previously described sites. The following trends emerge from Fig. 10a: in normally consolidated sands with no presence of microstructure, $G_{measured}/G_{estimated}$ is almost constant with K_D and ranges from 0.8 to 1.45, but most datapoints are grouped around 1. For soils with a significant presence of microstructure, no particular trend between $G_{measured}/G_{estimated}$ and K_D is observed. For these soils, $G_{measured}/G_{estimated}$ is larger than 1.8. In Fig. 10b, the relationship between $G_{measured}/G_{estimated}$ and I_D is shown. It can be observed that no particular trend exists between $G_{measured}/G_{estimated}$ and I_D for any type of soil.

The presented results indicate that the boundary separating soils with and without a significant presence of microstructure can be drawn at a ratio of $G_{measured}/G_{estimated}$ of 1.5. This is consistent with a reported 20% average relative error (e.g., Marchetti, 2014) in the estimated V_s from mechanical DMT, i.e., uncertainty emerging from local site conditions and soil variability are included in the proposed constant $G_{measured}/$

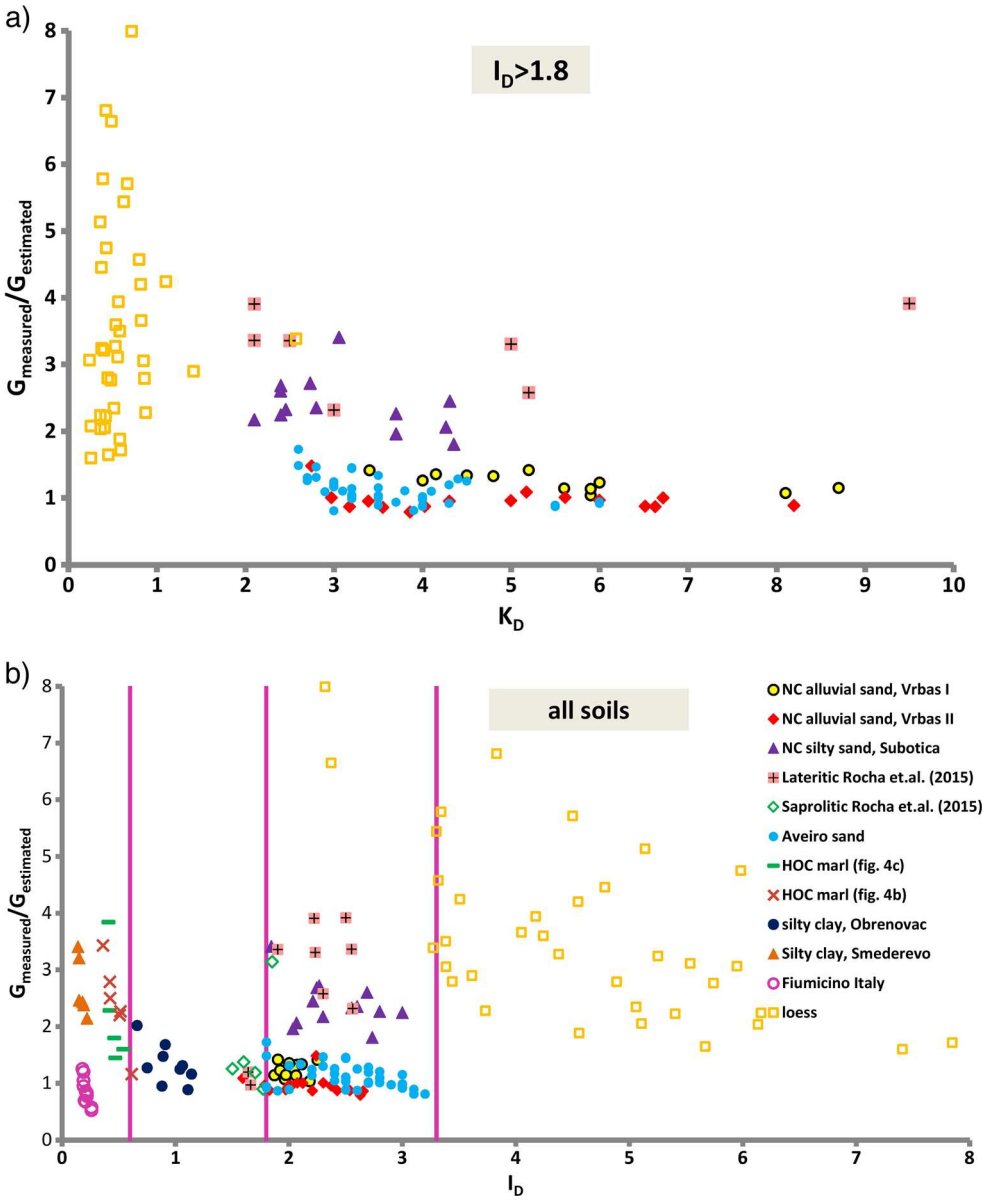

Fig. 10 Ratio of $G_{measured}/G_{estimated}$ versus (**a**) K_D for coarse-grained soils; and (**b**) I_D for various soil types

$G_{estimated}$ value that separates soils with and without a significant presence of microstructure.

Figure 11 shows the plot of the G_0/K_D ratio versus K_D on a log–log scale for all values of I_D. There is a clear tendency of decreasing G_0/K_D with increasing K_D.

It can be observed that coarse-grained soils tend to have a higher G_0/K_D ratio than fine-grained soils for the same value of K_D. However, the graph should not be used alone for determination of the presence of microstructure, since different soil types can overlap. An example is the position of Smederevo silty clay ($I_D < 0.6$) which has a high presence of microstructure plot within the region of NC Aveiro sand ($I_D > 1.8$) without microstructure. When compared, NC sands have different rates of decreasing G_0/K_D with K_D, with a higher rate for a sand in a looser state (higher ψ). It should be mentioned that this type of graph is not non-dimensional, since G_0 is in MPa. This makes the ordinate sensitive to changes in scale when different units for G_0 are used. However, the general trend of the G_0/K_D ratio decreasing with increasing K_D would be the same. No particular trend can be observed between G_0/K_D and I_D, except for the previously mentioned fact that coarse-grained soils have a higher G_0/K_D ratio than fine-grained soils.

Influence of microstructure on derived parameters

This section shows the results of comparison between the different methods used to derive axisymmetric effective peak

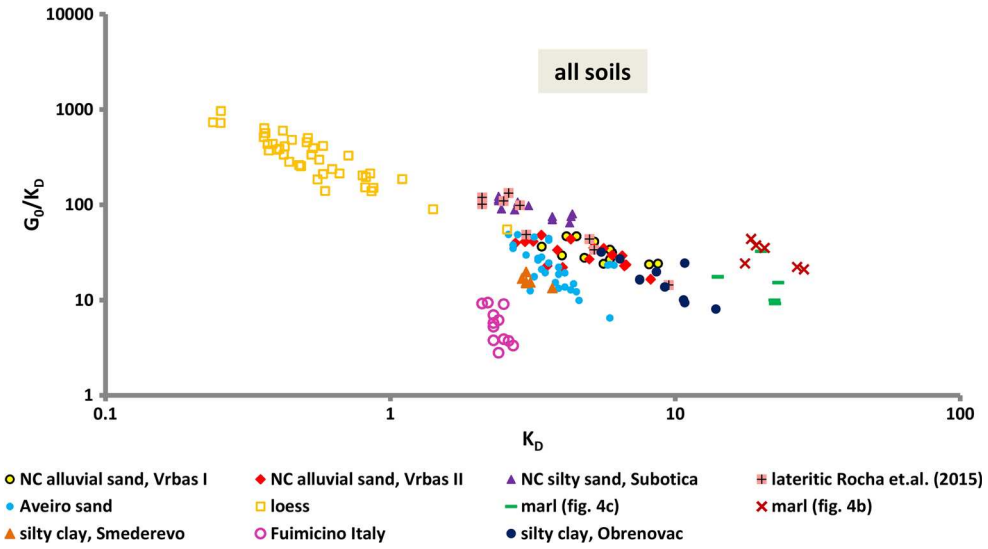

Fig. 11 Ratio of G_0/K_D versus K_D for various soil types. G_0 small strain stiffness

friction angles (φ_p') and the lateral stress coefficient at rest (K_0) for soils with and without significant presence of microstructure. Friction angles are derived from common correlations used for DMT and CPT interpretation in sands. The correlations with the respective equations used are shown in Table 1. Two DMT-based, two CPT-based, and one V_s-based correlations are used. The V_s was determined from an SDMT. The distance between the SDMT and CPT is approximately 1 m. All the mentioned correlations have been derived predominantly for quartz-silica sands from the results obtained in the calibration chamber (CC) or triaxial testing on undisturbed samples. Figure 12 shows the results obtained from the Vrbas II site.

For this site, CPT was performed to a depth of approximately 18 m. Figure 12 indicates the following:

- All correlations give a similar distribution of φ_p' with depth.
- The DMT- and CPT-based correlations predict similar values. The correlation proposed by Marchetti (1997) gives the lowest values of friction angles. This is consistent with the findings that φ_p' derived from K_D represents a lower bound value (see Marchetti et al. 2001; Mayne 2015).
- The highest φ_p' is predicted by the V_s-based approach. Uzielli et al. (2013) derived the correlation shown in Table 1 based on 12 datasets for the stress-normalized V_s in the range of 125–225 m/s. For the Vrbas II site, the majority of stress-normalized V_s are higher than 225 m/s or close to the upper boundary of 225 m/s. This may be one of the reasons for the inconsistency between φ_p' predicted from V_s and other applied correlations.
- The difference between φ_p' derived from D&M theory (Schmertmann, 1988) and from q_c (Kulhawy and Mayne, 1990) increases with increase in sand density. This difference is largest at depths from 11.6 to 13.2 m. Briaud and

Table 1 Origin of equations used for φ_p') determination (key in Figs. 12 and 13)

Approach based on	Equation	Reference
K_D (DMT)	$\varphi_p' = 28^\circ + 14.6\,log\,(K_D) - 2.1[log(K_D)]^2$	Marchetti (1997)
q_D (DMT)	$q_f = q_D = \gamma_s B N_{\gamma q} \xi_{\gamma q}$	Durgunoglu and Mitchell (1973); Schmertmann (1988)
D_r (CPT)[a]	$\varphi_p' = 34.5 + 0.1\{0.32\,ln\,[(q_c/p_a)/[17.68(\sigma_{v0}'/p_a)^{0.5}]]\}$	Jamiolkowski et al. (2001); Schmertmann (1978)
q_c (CPT)	$\varphi_p' = 17.6 + 11log[(q_c/p_a)/(\sigma_v'/p_a)]^{0.5}$	Kulhawy and Mayne (1990)
V_s (SDMT)	$\varphi_p'\,(degrees) = 3.9^\circ[V_s/(\sigma_v'/p_a)^{0.25}]^{0.44}$	Uzielli et al. (2013)

φ_p' secant axisymmetric effective peak friction angle, **σ_v'** vertical effective stress, **γ_s** average effective unit weight for the soil above the DMT blade, **$\xi_{\gamma q}$** shape factor, **B** thickness of DMT blade, *CPT* cone penetration test, *DMT* dilatometer test, **K_D** horizontal stress index, **$N_{\gamma q}$** bearing capacity factor, **p_a** atmospheric pressure, **q_c** cone resistance, **q_D** DMT penetration stress, **q_f** *D&M* Durgunoglu & Mitchell bearing capacity, *SDMT* seismic dilatometer, , **V_s** shear wave velocity

[a] General form of this equation is $\varphi_p' = a + b\{D_r\}$ (Schmertmann 1978). Coefficients a and b are 34.5 and 0.1, respectively (see Fig. 12 from Jamiolkowski 2001). Relative density (D_r) is estimated based on Eq. 5 proposed by Jamiolkowski et al. (2001). Coefficients C_0, C_1, and C_2 are 17.68, 0.5, and 3.1 respectively. These coefficients (see Table 4 in Jamiolkowski et al. 2001) represent average values for NC silica sands

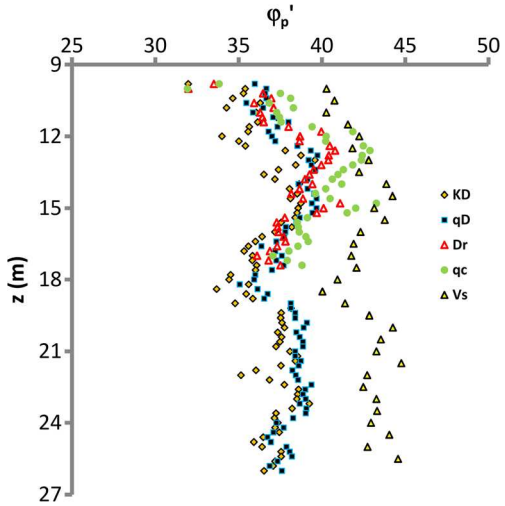

Fig. 12 Comparison of φ_p' derived from various methods (see Table 1) for Vrbas II site. $\boldsymbol{\varphi_p}$**'** secant axisymmetric effective peak friction angle, $\mathbf{K_D}$ horizontal stress index, $\mathbf{q_c}$ cone resistance, $\mathbf{q_D}$ dilatometer test penetration stress, $\mathbf{V_s}$ shear wave velocity, $\mathbf{D_r}$ relative density

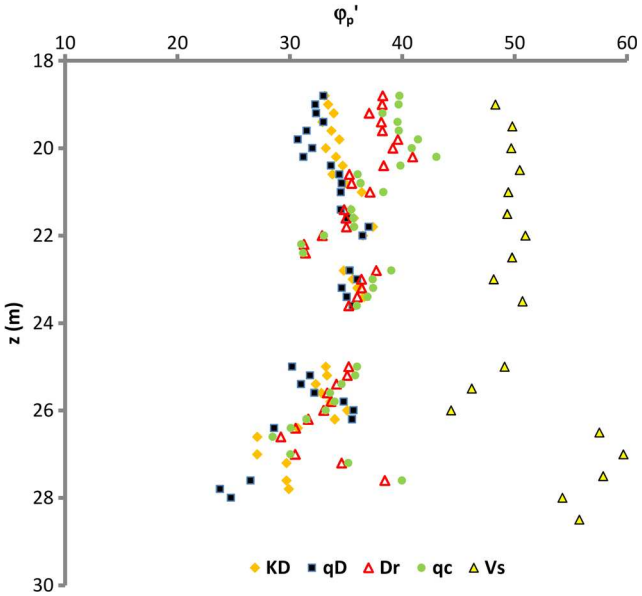

Fig. 13 Comparison of φ_p' derived from various methods (see Table 1) for Subotica site. $\boldsymbol{\varphi_p}$**'** secant axisymmetric effective peak friction angle, $\mathbf{K_D}$ horizontal stress index, $\mathbf{q_c}$ cone resistance, $\mathbf{q_D}$ dilatometer test penetration stress, $\mathbf{V_s}$ shear wave velocity, $\mathbf{D_r}$ relative density

Miran (1992), based on the research conducted by Jamiolkowski et al. (1988), mentioned that the difference between φ_p' laboratory (LAB) and φ_p' (D&M) increases with increasing sand density. Mayne (2014) and Mayne (2015) showed that the equation proposed by Kulhawy and Mayne (1990) correlates well with φ_p' (LAB) measured in triaxial compression tests. Thus, if φ_p' derived from Kulhawy and Mayne (1990) correlation is assumed to represent the LAB triaxial value, the greater difference between φ_p' obtained from q_c (LAB) and D&M in more dilative sand layers is confirmed.

– No correction for the failure envelope curvature is introduced in any of the presented φ_p' values. Thus, all values correspond to the mean normal effective stress existing around the blade or cone during penetration.

Figure 13 shows φ_p' values derived from the correlations shown in Table 1 for the NC Subotica silty sand. For this sand, the results indicate the following:

– The correlation proposed by Uzielli et al. (2013) significantly overpredicts φ_p' compared to any other used method. This signifies the importance of detecting the presence of microstructure in soil before using existing V_s-based empirical correlations. At this site, the V_{s1} values are significantly higher than 225 m/s, the upper bound value for which the method applies, as suggested by Uzielli et al. (2013).
– DMT-based methods (K_D and q_D) predict similar values of φ_p' when compared to each other. Higher values are obtained from CPT-based methods (Dr and q_c) than from DMT-based methods. This is most pronounced approximately between 18.5 and 20.2 m.

The presented results indicate that it is difficult to access the ultimate shear strength from tests that induce small shear strains in soil, such as when using V_s in order to determine φ_p'. The error is increased with increase in the presence of microstructure in the soil due to the sensitivity of V_s to it. In contractive sands (Subotica sand) cementation has a small influence on the measured penetration resistances (q_c, q_D, and K_D), which is governed by the sand density and stress state.

Some aspects of the derivation of K_0 in soils with a significance presence of microstructure are given below. Various methods for estimating K_0 in clay can be found in the literature (Kulhawy and Mayne 1990; Lacasse and Lunne 1988; Larsson 1989; Lunne et al. 1990; Marchetti 1980; Powel and Uglow 1988; Smith and Houlsby 1995; Sully 1991; Yu 2004). Kulhawy and Mayne (1990) proposed the general form of the equation for determining K_0 as:

$$K_0 = (K_D/\beta_K)^{0.47} - 0.6 \quad (2)$$

where parameter β_k depends on the soil type and geologic

Table 2 β_k parameter related to soil type (Kulhawy and Mayne 1990)

β_k	Soil type
0.9	Fissured clays
1.5 (Marchetti 1980)	Insensitive clays
2	Sensitive clays
3	Glacial till

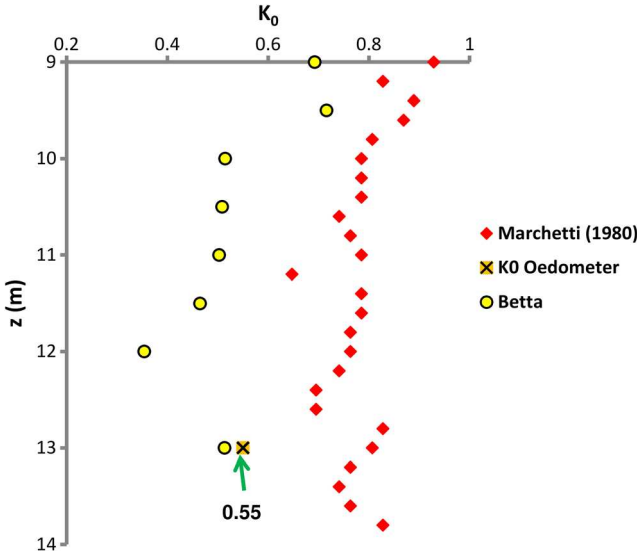

Fig. 14 Comparison of the lateral stress coefficient at rest (K_0) derived from seismic dilatometer (SDMT) and oedometer test results

origin (Kulhawy and Mayne 1990). For preliminary assessment of β_k, Kulhawy and Mayne (1990) recommend the values given in Table 2. Marchetti et al. (2001) states that in highly cemented clays the original equation ($\beta_k = 1.5$) can significantly overestimate K_0, since part of K_D is due to cementation. If we assume that β_k increases with cementation, which can be discerned from Table 2, the influence of cementation on the K_0–K_D correlation can be assessed by introducing the ratio of $G_{measured}/G_{estimated}$ to be equal to β_k in Eq. 2. This would ensure reducing the derived K_0 with the increasing presence of microstructure in clayey soil. Thus, Eq. 2 can be used with $b_k = G_{measured}/G_{estimated}$, with β_k ranging from 1.5 to 3 (as per Table 2). It is suggested to use this approach, named "Betta", for soils with $I_D < 0.6$. To illustrate this, a comparison between the original Marchetti (1980) correlation, using β_k = 1.5, and Eq. 2 with β_k depending on the microstructure, is shown in Fig. 14. The reference value derived from an oedometer with horizontal stress measurement is included in Fig. 14. It can be seen that K_0 predicted by Eq. 2 with varying β_k compares much better with the reference K_0 than the original Marchetti (1980) correlation. The proposed approach is sensitive to variation of the $G_{measured}/G_{estimated}$ ratio. At 12.0 m, the $G_{measured}/G_{estimated}$ ratio is higher than 3. In this case, β_k equal to 3 should be used in Eq. 2, giving the lowest K_0 value in the profile of 0.35. Nevertheless, most data below 10.0 m are close to the reference value of 0.55.

Comparison of DMT and Cone penetration test with pore pressure measurement (CPTu) SBT charts in marls

Robertson (2016) showed that Seismic cone penetration test with pore pressure measurement (SCPTu) results in soils with significant microstructure can be described differently by soil behavior type-normalized (SBTn) Q_{tn}–F_r and Q_{tn}–U_2 charts. To illustrate this, results for very stiff, HOC Belgrade marl are shown in Fig. 15 on Q_{tn}–F_r and Q_{tn}–U_2 charts. The SCPTu data from 22 to 26 m plot in the dilative-sand region (SD) of the Q_{tn}–F_r chart and the claylike-contractive (CC) of the Q_{tn}–U_2 chart. High Q_{tn} value is caused by high apparent OCR, suggesting possible dilative behavior, where high U_2 shows a more contractive behavior at high shear strains consistent with cemented soils. Results presented here are somewhere between results obtained in Cooper Marl and Fernando Siltstone (soils with reference number 28 and 29 from Robertson 2016). On the other hand, SDMT data for marls (similar to Belgrade marl) plot in the fine-grained-dilative (FD) region, as shown in Fig. 6. Thus, the two most common

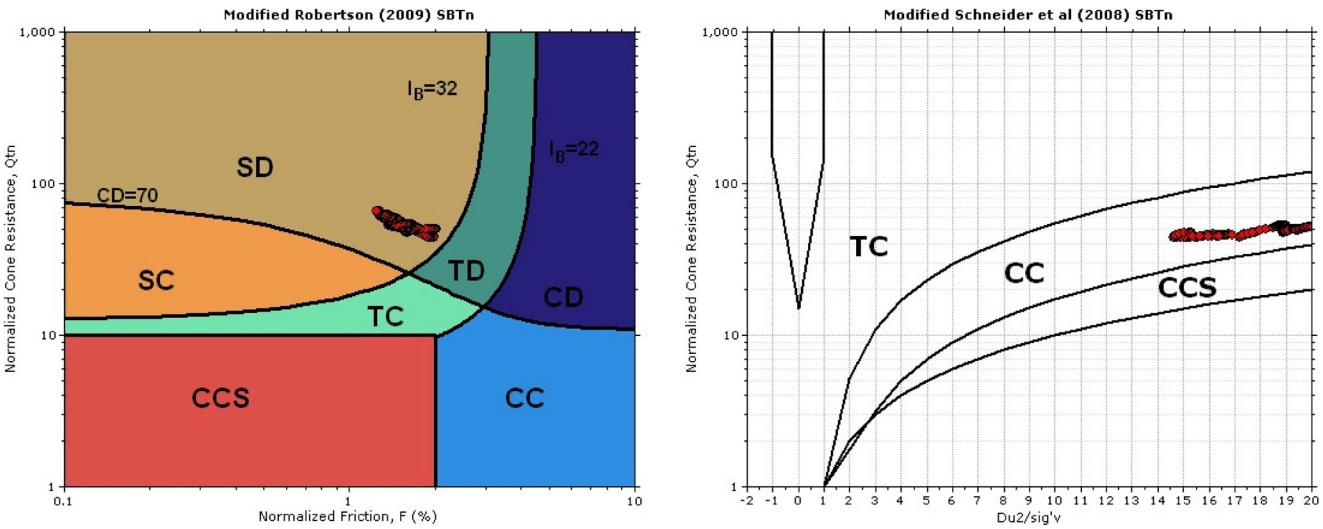

Fig. 15 Normalized (CPTu) cone penetration test with pore pressure measurement data from 22 to 26 m obtained in HOC Belgrade marl

field tests, SCPTu and SDMT, provide three different descriptions of marls (SD, CC, and FD) based on their behavior response during penetration and testing. These differences can be attributed to a different operational shear strain level induced by cone and the blade during penetration. It should be emphasized that CPTu-based soil behavior type charts, which have been used for some time now, can give valuable insight into recently developed DMT-based soil behavior type charts.

Conclusion

This paper indicates the possibility of using SDMT results for soil type evaluation and determining the presence of microstructure. The intermediate parameters I_D and K_D are used for soil type determination, while the G_0/σ_v' ratio is used to determine the presence of microstructure in a soil. Four broad groups of soil types, as shown in Fig. 5, are distinguished based on their response to DMT blade insertion and membrane expansion. It is shown that the G_0/σ_v' ratio can effectively be used to distinguish between soils with and without the presence of microstructure. It is found that the difference between the measured and estimated G_0/σ_v' ratio increases with increasing presence of microstructure. The boundary that separates soils with and without microstructure is found to be at the ratio of $G_{0measured}/G_{0estimated}$ of 1.5. The ratio of $G_{0measured}/G_{0estimated}$ is highest in macroporous loess, lateritic soils, and marls, which are soils well-known to have a high presence of microstructure. The lowest ratio is found in NC Fiumicino clay and clean quartz sands. Direct comparison of measured and estimated V_s is an equally good way to detect the presence of microstructure in a soil. If the relative error between the measured and estimated V_s is more than 20%, the soil may have microstructure. Direct use of the correlations proposed by Marchetti et al. (2008) for G_0/M_{DMT} evaluation using K_D and I_D is applicable only if the soil is known to have a low presence of microstructure. It is shown that the G_0/K_D ratio decreases with increasing K_D. Coarse-grained soils tend to have a higher G_0/K_D ratio for the similar range of $G_{0measured}/G_{0estimated}$. The applicability of the V_s or G_0/σ_v' ratio to detect the presence of microstructure in transitional soils ($0.6 < I_D < 1.8$) still needs to be confirmed.

For quartz-silica sands without microstructure, the common correlations (derived for quartz-silica sands) used to obtain the effective peak axisymmetric friction angle (φ_p') from DMT and CPT can be used with confidence. This observation is based on the similarity and small variation of the estimated φ_p' with all the correlations used. The V_s-based approach predicts higher values of φ_p' than the other methods used in quartz-silica sands. In sands with a high presence of microstructure, φ_p' predicted from V_s is overly high and should not be used in design. We present an idea of reducing K_0 by taking into account the influence of microstructure on K_D. It is suggested that the $G_{0measured}/G_{0estimated}$ ratio be used as a divisor in Eq. 2 instead of a constant value of 1.5. If no presence of microstructure is found in the soil ($\beta_k = G_{0measured}/G_{0estimated} = 1.5$), Eq. 2 becomes identical to the original Marchetti (1980) equation. The lower and upper bounds of $G_{0measured}/G_{0estimated}$ used in Eq. 2 are 1.5 and 3, respectively. This approach is applicable for soils with $I_D < 0.6$.

References

Alonso EE, Gens A, Josa A (1990) A constitutive model for partially saturated soils. Geotechnique 40(3):405–430

Amoroso S, Rodrigues C, Viana da Fonseca A, Cruz N (2015) Liquefaction evaluation of Aveiro sands from SCPTU and SDMT Tests. Proceedings of the 3rd International Conference on the flat dilatometer DMT'15, Roma, pp 293–300

Andrus RD, Hayati H, Mohanan NP (2009) Correcting liquefaction resistance for Aged Sands using measured to estimated velocity ratio. J Geotech Geoenviron 135(6):735–744

Wen B-P, Yan Y-J (2014) Influence of structure on shear characteristics of the unsaturated loess in Lanzhou, China. Eng Geol 168:46–58

Berisavljevic D, Berisavljevic Z, Čebašek V, Šušić N (2014) Characterisation of collapsing loess by seismic dilatometer. Eng Geol 181:180–189

Berisavljevic D, Rakic D, Susic N, 2015. SDMT – a tool for in situ identification of collapsible soils. Proceedings of the 3rd International Conference on the Flat Dilatometer DMT'15, Roma, pp 457–463

Briaud JL, Miran J (1992) The flat dilatometer test. Department of Transportation - Federal Highway Administration, Washington, DC. Publication No. FHWASA-91-044, p 102

Burland JB (1990) On the compressibility and shear strength of natural clays. Geotechnique 40(3):329–378

Campanella RG, Robertson PK (1991) Use and interpretation of research dilatometer. Can Geotech J 28:113–126

Cotecchia F, Chandler RJ (1997) The influence of structure on the pre-failure behaviour of a natural clay. Geotechnique 47(3):523–544

Cruz N, Rodrigez C, Viana da Fonseca A (2012) Detecting the present of cementation structures in soils, based in DMT interpreted charts. In: Couthino, Mayne (eds) In geotechnical and geophysical site characterization. Taylor and Francis group, London, pp 1723–1728

Cuccovillo T, Coop MR (1997) Yielding and pre-failure deformation of structured sands. Geotechnique 47(3):491–508

Devincenzi MJ, Canicio M (2001) Geotechnical characterization by in situ tests of a loess-like deposit in its natural state and after saturation. Proceedings of the International Conference on In-Situ Measurement of Soil Properties and Case Histories, Bali, Indonesia, 159–166

Diaz-Rodriguez JA, Santamarina JC (2001) Mexico City soil behavior at different strains: observations and physical interpretation. J Geotech Geoenviron Eng 127(9):783–789

Durgunoglu TH, Mitchell JK (1973) Static penetration resistance of soils. Prepared for NASA Headquarters, Washington, D. C. under NASA Grant NGR 05–003-406, "Lunar Soil Properties and Soil Mechanics"

Fernandez A, Santamarina JC (2001) Effect of cementation on the small strain parameters of sands. Can Geotech J 38(1):191–199

Gasparre A, Coop MR (2008) Quantification of the effects of structure on the compression of a stiff clay. Can Geotech J 45:1324–1334

Giacheti HL, Peixoto ASP, De Mio G, Carvalho D (2006) Flat dilatometer testing in Brazilian tropical soils. In: Failmezger RA, Anderson JB (eds). Second International Conference on the Flat Dilatometer, Washington. Vol. 1. ASCE, Washington, DC p 103–110

Hayati H, Andrus RD (2009) Updated liquefaction resistance correction factors for Aged Sands. J Geotech Geoenviron 135(11):1683–1692

Heineck KS, Coop MR, Consoli NC (2005) Effect of microreinforcement of soils from very small to large shear strains. J Geotech Geoenviron 131(8):1024–1033

Jamiolkowski M, Ghionna V, Lancellotta R, Pasqualini E (1988) New Correlations of Penetration Tests for Design Practice. Proc. ISOPT-1, Orlando, Florida,z 1:263–296

Jamiolkowski M, Lo Presti DCF, Manassero M (2001) Evaluation of relative density and shear strength of sands from cone penetration test (CPT) and flat dilatometer test (DMT). ASCE Geotechnical Spec Publ 119:201–238

Jiang M, Zhang F, Hu H, Cui Y, Peng J (2014) Structural characterization of natural loess and remolded loess under triaxial tests. Eng Geol 181:249–260

Jotisankasa A, Ridley A, Coop MR (2007) Collapse behavior of compacted Silty clay in suction-monitored Oedometer apparatus. J Geotech Geoenviron 133(7):867–877

Kulhawy FH, Mayne PW (1990) Estimating soil properties for foundation design. EPRI report EL-6800. Palo Alto, Electric Power Research Institute, p 306

Lacasse S, Lunne T (1988) Calibration of dilatometer correlations. Proceedings of ISOPT-1, Orlando, FL, Vol. 1, 539–548

Lambe TW, Whitman RV (1969) Soil mechanics. John Wiley & Sons Inc., New York

Larsson R (1989) Dilatometerförsök (dilatometer tests) [in Swedish]. Swedish Geotechnical Institute, Information No. 10, Linköping

Leroueil S, Vaughan PR (1990) The general and congruent effects of structure in natural soils and weak rocks. Geotechnique 40(3): 467–488

Lunne T, Powell JJM, Hauge EA, Uglow IM, Mokkelbost KH (1990) Correlation of dilatometer readings to lateral stress. Paper submitted to specialty session on measurement of lateral stress. 69th Annual Meeting of the Transportation Research Board, Washington, DC

Lutenegger AJ, Donchev P (1983) Flat dilatometer testing in some metastable loess soils. Proc Int Symp In-Situ Testing Soil Rock Properties 2:337–340

Marchetti S (1980) In situ tests by flat dilatometer. J Geotech Eng 106(3): 299–321

Marchetti S (1997) The flat dilatometer: design applications. Proceedings of the Third International Geotechnical Engineering Conference, Cairo University, Soil Mechanics and Foundation Research Laboratory, Egypt: 423–448

Marchetti S (2014) The seismic dilatometer for in situ soil investigations. Proceedings of the Indian Geotechnical Conference IGC-2014, Kakinada, India

Marchetti S (2015) Some 2015 updates to the TC16 DMT report 2001. Proceedings of the 3rd International Conference on the Flat Dilatometer DMT'15, Roma, pp 43–65

Marchetti S, Monaco P, Totani G, Calabrese M (2001) The flat dilatometer (DMT) in soil investigations (ISSMGE TC16). Proceedings of the International Conference on In-Situ Measurement of Soil Properties and Case Histories, Bali, Indonesia, 95–131

Marchetti S, Monaco P, Totani G, Marchetti D (2008) In situ tests by seismic dilatometer (SDMT). In Laier JE, Crapps DK, Hussein MH (eds), From research to practice in geotechnical engineering, ASCE Geotech. Special Publication No. 180 (honoring Dr. John H. Schmertmann), pp 292–311

Mayne PW (2015) Peak friction angle of undisturbed sands using DMT. 3rd International Conference on the Flat Dilatometer DMT'15, Roma, pp 237–242

Mayne PW (2014) Interpretation of geotechnical parameters from seismic piezocone tests. Proceedings of the 3rd International Symposium on Cone Penetration Testing, Las Vegas, Nevada, 47–73

Mlynarek Z, Wierzbicki J, Manka M. (2015) Geotechnical parameters of loess soils from CPTU and SDMT. Proceedings of the 3rd International Conference on the flat dilatometer DMT'15, Roma, pp 481–488

Monaco P, Marchetti S, Totani G, Marchetti D (2009) Interrelationship between small strain modulus G0 and operative modulus. In: Kokusho T, Tsukamoto Y, Yoshimine M (eds) Performance-based Design in Earthquake Geotechnical Engineering- from case history to practice, proc. IS-Tokyo 2009, Tsukuba, Japan, June 15–17. Taylor & Francis Group, London (CD-Rom), pp 1315–1323

Mulabdic M, Minazek K (2015) Use of dilatometer in unusual difficult soils – a case study. Proceedings of the 3rd International Conference on the Flat Dilatometer DMT'15, Roma, pp 497–504

Ortigao JAR (1994) Dilatometer tests in Brasilia porous clay. 7th International Congress of the International Association of Engineering Geology, Lisbon, Portugal

Ortigao JAR, Cunha RP, Alves LS (1995) In situ tests in Brasilia porous clay. Can Geotech J 33:189–198

Pestana JM, Salvati LA (2006) Small-strain behavior of granular soils. I: model for cemented and Uncemented Sands and gravels. J Geotech Geoenviron 132(8):1071–1081

Powell JJM, Uglow IM (1988) The interpretation of the Marchetti Dilatometer Test in UK clays. ICE Proceedings of the Conference on Penetration Testing in the UK, University of Birmingham, Paper No. 34, 269–273

Rinaldi VA, Redolfi ER, Santamarina JC (1998) Characterization of collapsible soils with combined geophysical and penetration testing. Proceedings of the First International Conference on Site Characterization, ISC '98, vol. 1, Atlanta (GA)

Rinaldi VA, Santamarina JC (2008) Cemented soils: small strain stiffness. In: Burns, Mayne and Santamarina (eds) IOS-Millpress. Deformational Characteristics of Geomaterials 1:267–274

Rivera-Cruz I, Howie J, Vargas-Herrera LA, Coto-Loria M, Luna-Gonzalez O (2012) A new approach for identification of soil behaviour type from seismic dilatometer (SDMT) data. In: Couthino, Mayne X (eds) In geotechnical and geophysical site characterization. Taylor and Francis group, London, pp 947–954

Robertson PK (2010) Estimating in-situ state parameter and friction angle in sandy soils from CPT. 2nd International Symposium on Cone Penetration Testing, CPT'10, Huntington Beach (CA)

Robertson PK (2012) Interpretation of in-situ tests – some insights. J.K. Mitchell Lecture, Proceedings of the 4th International Conference on Site Characterization, ISC'4, Porto de Galinhas, Brazil, 3–24

Robertson PK (2015) Soil behavior type using the DMT. Proceedings of the 3rd International Conference on the Flat Dilatometer DMT'15, Roma, pp 243–250

Robertson PK (2016) Cone penetration test (CPT)-based soil behaviour type (SBT) classification system — an update. Can Geotech J 53: 1910–1927

Rocha BP, Castro BAC, Giacheti GL (2015) Seismic DMT Test in a non-text book type geomaterial. Proceedings of the 3rd International Conference on the Flat Dilatometer DMT'15, Roma, pp 505–512

Sally JP (1991) Measurement of in situ lateral stress during full displacement penetration tests [Ph.D. Thesis]. University of British Columbia, Vancouver, BC, pp 485

Schmertmann JH (1978) Guidelines for cone penetration test, performance and design. Report FHWA-TS-78-209, Washington, 145

Schmertmann JH (1988) Guidelines for using the CPT, CPTU and Marchetti DMT for geotechnical design. U.S. Department of Transportation, Federal Highway Administration, Office of Research and Special Studies, Report No. FHWA-PA- 87 023+24, Vol. 3–4

Schnaid F (2005) Geo-characterisation and properties of natural soils by in situ tests. Proceedings of the 16th International Conference on Soil Mechanics and Geotechnical Engineering, vol. 1, Osaka, Millpress, Rotterdam, pp 3–45

Schnaid F, Odebrech E (2015) Challenges in the interpretation of the DMT in tailings. Proceedings of the 3rd International Conference on the Flat Dilatometer DMT'15, Roma, pp 13–23

Schneider JA, Moss RES (2011) Linking cyclic stress and cyclic strain based methods for assesment of cyclic liquefaction triggering in sands. Geotechnique Lett 1:31–36

Smith MG, Houlsby GT (1995) Interpretation of the Marchetti dilatometer in clay. Proc 11th ECSMFE 1:247–252

Uzielli M, Mayne PW, Cassidy MJ (2013) Probabilistic assessment of design strengths for sands from in-situ testing data, Modern geotechnical design codes of practice, advances in Soil Mechanics & Geotechnical Engineering (series), vol 1. IOS Millpress, Amsterdam, pp 214–227

Viana da Fonseca A, Carvalho J, Ferreira C, Santos JA, Almeida F, Pereira E, Feliciano J, Grade J, Oliveira A (2006) Characterization of a profile of residual soil from granite combining geological, geophysical and mechanical testing techniques. Geotech Geol Eng 24:1307–1348

Yamamuro JA, Wood FM, Lade PV (2008) Effect of depositional method on the microstructure of silty sand. Can Geotech J 45:1538–1555

Yu HS (2004) In situ soil testing: from mechanics to interpretation. 1st J. K. Mitchell Lecture, Proceedings of ISC-2, Porto. 1, 3–38

Yun TS, Santamarina JC (2005) Decementation, softening, and collapse: changes in small-strain shear stiffness in k0 loading. ASCE J Geotech Geoenviro Eng 131(3):350–358